

Low-Viscosity Measurement by Capillary Electromagnetically Spinning Technique

Maiko Hosoda*, Taichi Hirano¹, and Keiji Sakai¹

Tokyo Denki University, Hatoyama, Saitama 350-0394, Japan

¹*Institute of Industrial Science, University of Tokyo, Meguro, Tokyo 153-8505, Japan*

Received December 11, 2010; accepted March 2, 2011; published online July 20, 2011

We study sphere rotation against viscous torque confined in a small space. Our new invention, the electromagnetically spinning sphere (EMS) viscometer measures liquid viscosity through the observation of sphere rotation driven by electromagnetic interaction in a noncontact manner. The lower limit of the measurable viscosity is determined from the ratio between the viscous torque and the mechanical friction, and the apparent increase in the contribution of the viscous term leads to the improvement of the accuracy of low-viscosity measurement. We propose a theoretical expression of the torque applied to a sphere rotating in a cylinder and obtained the power law with respect to the gap in between. The results of the numerical simulation and experiment provide evidence of the validity of the theory. © 2011 The Japan Society of Applied Physics

1. Introduction

Viscoelasticity is one of the important properties of soft condensed materials representing its dynamic response against mechanical stimulation.¹⁻³⁾ Generally, viscosity and elasticity are variables that depend on the speed of medium deformation, the behavior of which is often represented in terms of two aspects: rheology and ultrasonic spectroscopy. These two studies require different measurement techniques, but share the same concept that the viscoelasticity should be represented as a function of the frequency or the inverse of the deformation time.

Rheology has a technical advantage over ultrasonic spectroscopy in the sense that it can measure viscosity as low as 10^{-3} Pa·s, which approximates that of pure water. The ultrasonic absorption due to the shear viscosity of water is on the order of 10^{-2} m⁻¹ at 1 MHz, which is too small to be accurately observed. The measurement of such a low ultrasonic absorption requires a sophisticated resonance method.^{4,5)}

It is also important that the rheology measurement determines the low-frequency limit of the ultrasonic propagation in materials with different measurement techniques; complementary use of the two techniques is effective for studying the mechanical science of materials. On the other hand, the ultrasonic propagation can derive information on fast molecular dynamics up to the GHz frequency range.⁶⁻¹⁰⁾ To be honest, from the standpoint of a rheologist, however, the measurement of low viscosity is still difficult also for rheology at present.

In this paper, we introduce a method of measuring viscosity of as low as 1 mPa·s, which is that of pure water. The suppression of the rotation of a sphere confined in a small space was theoretically analyzed, and the result was applied to the newly developed viscosity measurement system.

2. Measurement of Low Viscosity

The electromagnetically spinning sphere (EMS) viscometer is our recent invention, which allows easy measurement of viscosity depending on the shear deformation rate.¹¹⁾ Here, we briefly describe the principle of the EMS viscometer. A metal sphere is immersed in the sample, which works as a probe of the viscosity. A magnetic field rotating in the

horizontal plane with a magnitude of 100 mT is applied to the sphere, and the Lorentz interaction between the induced current and the magnetic field works so that the sphere rotates following the rotation of the magnetic field. The relationship between the applied torque and the revolution speed gives the viscosity as a function of the sphere rate. The measurement range of the viscosity is 10^{-3} – 10^1 Pa·s, the upper limit of which depends on the patience of the operator given the long measurement time, while the lower limit is determined by the harm from the friction between the probe sphere and the cell bottom.

We are trying to expand the measurement range towards both lower and higher viscosities. In this paper, we describe the application of EMS to the measurement of low viscosities, in which the contribution of the viscous effect is enhanced by confining the probe sphere within a small space.

Aqueous solutions of materials are certainly important for the chemical industry as well as bioengineering. The viscosity of the solution is generally higher than that of the solvent, and the resolution of 10% at the viscosity $\eta = 1$ mPa·s would be sufficient for the application to the above promising industrial fields.

The lower limit of viscosity measurable with the EMS system is determined under the condition that the torque due to the surrounding viscosity should overcome that of the friction between the bottom of the probe sphere and the sample cell. The former is proportional to the third power of the sphere radius, while the latter is proportional to the fourth power, and the condition holds for a satisfactorily small sphere. As for the measurement of the viscosity of pure water at the sphere rotation of 10 rps, a radius of 1 mm for an aluminum sphere is the boundary of the condition. It shows, in other words, that the viscosity of water cannot be determined with satisfactory accuracy using the present EMS system.

The following is our idea to enhance the effect of viscosity by confining the probe sphere into a small space. The purpose of the discussion below is to find the scaling law of the enhancement factor depending on the gap distance between the sphere and the surrounding wall. To solve the problem, we consider the flow field of the medium around the spinning sphere at the bottom of the cell. The steady flow field around the sphere set in infinite medium is analytically given as¹²⁾

*E-mail address: mhosoda@mail.dendai.ac.jp

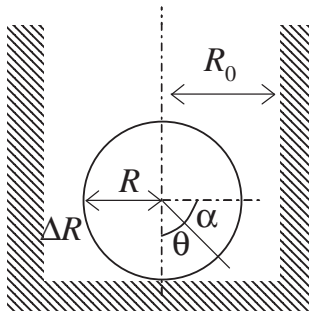


Fig. 1. Schematic of the geometry used in the calculation.

$$v_\phi = \Omega \sin \theta \left(\frac{R^3}{r^2} \right), \quad v_\theta = 0, \quad v_r = 0, \quad (1)$$

where R is the sphere radius and Ω is the angular velocity of the sphere. The polar coordinate is taken so that $\theta = 0$ and π correspond to the sphere bottom and top, respectively, and the geometry is schematically shown in Fig. 1. Note here that the nonzero component of the fluid velocity is v_ϕ , which is independent of ϕ from the rotational symmetry with respect to the center axis and $\partial/\partial\phi = 0$. Therefore, the divergence in the fluid flow that is given by

$$\text{div } \mathbf{v} = \frac{\partial v_r}{\partial r} + \frac{1}{r} \frac{\partial v_\theta}{\partial \theta} + \frac{1}{r \sin \theta} \frac{\partial v_\phi}{\partial \phi} + \frac{2v_r}{r} + \frac{v_\theta \cot \theta}{r}, \quad (1)$$

is calculated to be kept zero throughout and an incompressible condition strictly holds. The tangential component of the stress tensor is given as

$$\sigma_{r\phi} = \eta \left(\frac{\partial v_\phi}{\partial r} - \frac{v_\phi}{r} \right). \quad (2)$$

By substituting eq. (1) to eq. (2), we obtain the viscous torque applied to the surface area of the sphere between θ and $\theta + d\theta$ as

$$T(\theta) d\theta = 6\pi\eta\Omega R^3 \sin^3 \theta d\theta, \quad (3)$$

and the whole torque is then calculated as $M = 8\pi\eta R^3 \Omega$.

It would be worth referring to the stability of this flow system. The Reynolds number of the flow is roughly given by $Re = R^2 \Omega \rho / \eta$, which is as high as 100 for the low viscosity of 1 mPa·s at the rotational speed of $\Omega = 100 \text{ s}^{-1}$. The system thus safely remains in the layer flow even at such a high rotation; however, it might undergo transition to the turbulent flow hereafter. Actually, at $\Omega > 200 \text{ s}^{-1}$, the sphere rotating in pure water shows irregular fluctuation in its position. It is an advantage that the stability of the flow can be examined directly from the motion of the rotating sphere. Note here that the Reynolds number for the flow in the confined space becomes small, since the spatial length decreases.

Here, let us consider the effect of the bottom in contact with the sphere. In the vicinity of the bottom, where $\theta = 0$, the sphere surface is approximated to the parabola. The shear rate at the gap of the sphere and the bottom is $\gamma = 2\Omega / \sin \theta$, and the viscous torque is calculated as

$$T'(\theta) = 4\pi\eta R^3 d\theta \sin \theta d\theta. \quad (4)$$

In the actual system, the torque $T'(\theta)$ should be analytically connected to $T(\theta)$ as θ increases towards $\theta = \pi/2$.

We can show with the above formulas that the torque applied to the surface area in the vicinity of the sphere equator is dominant as the resistant torque due to the viscosity. The excess amount of $T'(\theta)$ over $T(\theta)$ would give a rough estimation of the contribution from the bottom effect to the whole viscosity torque, which is found to be as large as 1/10 from the numerical calculation. Another important finding obtained from the numerical approach to the flow field is that the torque applied to the region of $\pi/4 < \theta < 3\pi/4$ is more than 3/4 of the total torque.

It would, therefore, be a simple idea to emphasize the viscous resistant torque for the low-viscosity sample, that is, the shear deformation rate is increased by confining the sphere in the thin cylinder. The shear deformation rate around the sphere given by $\gamma = (\partial v_\phi / \partial r - v_\phi / r)$ is $\gamma = 3\Omega \sin^3 \theta / r^3$ in the present case, which reaches roughly as far as the distance R from the sphere surface. By restricting the space of the medium flow by inducing a thin cylinder with diameter $R + \Delta R$, the apparent torque due to the viscosity would increase by a factor of $(R/\Delta R)^\delta$, δ being the critical exponent.

Let us roughly estimate the torque applied to the sphere confined in a cylinder with the inner diameter $R + \Delta R$. Hereafter, we ignore the effect of the bottom of the sample cell, and the angle α is taken as $\alpha = \theta - \pi/2$.

It would be natural to consider that the shear deformation in the gap between the sphere and the cylinder is dominant to determine the torque. The gap decreases with increasing α and we cut off the integration of the torque up to the angle α_c , which gives the gap of $(1 + \beta)\Delta R$, β being a constant on the order of unity. The cutoff angle α_c is then given by $R(1 - \cos \alpha_c) = \Delta R$. It indicates that the sphere is approximated to a disk with the radius R and the thickness $D = 2R \sin \alpha_c$, and with the condition of $\Delta R \ll R$, D is given by $D = \sqrt{8R \cdot \Delta R}$. By applying this relation to the above approximated cylinder, we obtain the torque working on the sphere as $T \approx 4\sqrt{2}\pi R^3 \sqrt{(R/\Delta R)} \eta \Omega$. The result shows that the torque increases with decreasing gap as $T \propto (R/\Delta R)^{1/2}$ and $\delta = 1/2$. Roughly, the value of $\Delta R = R/10$ apparently enhances the viscous torque by a factor of $\sqrt{10}$.

Later, we give the results of the experimental examination of this critical exponent of 1/2. However, before describing the experimental results using the actual system, we carried out the numerical flow simulation using a commercially available software, FLOW-3D, and observed the behavior of a rotating sphere and a cylinder in a confined space. As for the cylinder, the solution of the analytical calculation in a two-dimensional system can be easily obtained, and the numerical simulation reproduces the critical exponent of -1.0 with respect to $(\Delta R/R)$ in the range of $\Delta R/R < 0.1$. The rotation of the sphere, on the other hand, shows the exponent of -0.5 also in the range as expected from the scaling theory. Note here that we do not take into account the contribution of the friction between the probe and the cell in the numerical study. Therefore, we have to examine the validity of the theory through an experiment using the actual measurement system.

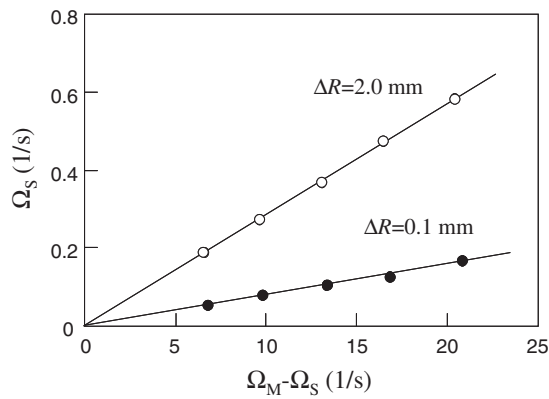


Fig. 2. Relationship between the sphere rotation Ω_s , and the difference between the rotational speed of the magnetic field and the probe sphere ($\Omega_M - \Omega_s$), obtained for the gap of $\Delta R = 0.1$ (closed circle) and 2.0 (open circles) mm.

3. Experimental Methods

To examine first the suppression of the rotation of the sphere confined in a small space, we prepared a cylinder made of polymer with an inner diameter of 2.1 mm, whereas the sphere is made of aluminum and has a diameter of 2.0 mm. The temperature is kept at $25 \pm 0.1^\circ\text{C}$ by a peltier-type thermostatic controller. The temperature increase due to the ohmic heat of the Lorentz current is estimated to be less than $1/100^\circ\text{C/s}$, which is negligible in the present experiment.

Figure 2 shows the rotational speed of the sphere Ω_s depending on the difference between the revolution of the magnetic field and the sphere ($\Omega_M - \Omega_s$), which is proportional to the applied torque. The results obtained for the sphere in a 2.1-mm-diameter cylinder and the usual sample tube of 6.0 mm diameter are represented by the closed and open circles, respectively. The sample is the viscosity standard liquid of $\eta = 1.0 \text{ Pa}\cdot\text{s}$, which was purchased from Shinetsu Silicone and was used without further purification. Here, we employed a rather viscous liquid since the contribution of the friction should be relatively neglected; the frictional torque is estimated to be less than $1/1000$ of that of the viscous resistance at the sphere rotation of 1.0 rad/s .

As shown in Fig. 2, the rotation in the thin cylinder is apparently slower than that in a free space owing to the effect of the wall in the vicinity of the sphere surface, and the ratio of suppression is about 3.7, which roughly agrees with the value of $\sqrt{R/\Delta R} \approx 3$. We refer hereafter to the ratio as the suppression factor. The result shows that the thin cylinder successfully enhances the torque owing to the sample viscosity. It would then be possible to improve the accuracy and the resolution of the measurement for the low-viscosity liquids.

Next, we examined the dependence of the suppression factor on the gap; cylinders of 2.1, 2.4, 3.0, and 4.0 mm inner diameter were prepared. Figure 3 shows the suppression factor of the sphere rotation plotted against the gap distance normalized by the sphere diameter. In the logarithmic plot,

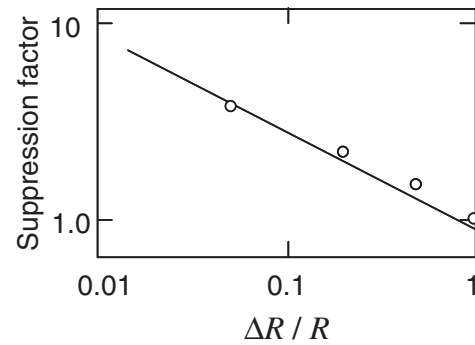


Fig. 3. Suppression factor describing the apparent increase in the viscous torque plotted against the gap distance. The solid line shows the theoretically predicted power law of $\delta = -1/2$.

the data shows the linear relation suggesting the power law on $\Delta R/R$. The solid line shows the relation of $-1/2$ the power of $(\Delta R/R)$, and the experimental results are well fitted by the line. We consider from the results that the viscous effect can be enhanced by confining the probe rotator in a small space, and the factor of the enhancement critically increases as $\Delta R/R$ approaches zero.

In conclusion, we obtained the power law describing the effect of the free space size on the apparent viscosity applied to the rotating object. It would directly lead to the improvement of the accuracy in the low-viscosity measurement. The apparent viscous effect applied to the object confined in a small space is also important to determine the fluctuation in the structure, such as the Brownian motion.¹³⁾ The results obtained in this study would be valuable in the field of physical property measurement based on the fluctuation–dissipation theory.

Acknowledgement

This work was partially supported by a Grant-in-Aid for Scientific Research from the Ministry of Education, Culture, Sports, Science and Technology.

- 1) D. S. Viswanath, T. K. Ghosh, D. H. L. Prasad, N. V. K. Dutt, and K. Y. Rani: *Viscosity of Liquid* (Springer, Dordrecht, 2007) p. 9.
- 2) T. Ueda: *Jpn. J. Appl. Phys.* **47** (2008) 3783.
- 3) A. Takeuchi, T. Yamada, and K. Sakai: *Jpn. J. Appl. Phys.* **49** (2010) 07HB12.
- 4) Y. Naito, P.-K. Choi, and K. Takagi: *J. Phys. E* **18** (1985) 13.
- 5) P.-K. Choi, Y. Naito, and K. Takagi: *J. Acoust. Soc. Am.* **74** (1983) 1801.
- 6) S. Kojima: *Jpn. J. Appl. Phys.* **49** (2010) 07HA01.
- 7) M. Kawabe, M. Matsukawa, and N. Ohtori: *Jpn. J. Appl. Phys.* **49** (2010) 07HB05.
- 8) K. Tanigaki, T. Kusumoto, H. Ogi, N. Nakamura, and M. Hirao: *Jpn. J. Appl. Phys.* **49** (2010) 07HB01.
- 9) H. Ogi, T. Shagawa, N. Nakamura, M. Hirao, H. Odaka, and N. Kihara: *Jpn. J. Appl. Phys.* **48** (2009) 07GA01.
- 10) M. Maebayashi, A. Shirai, Y. Asano, and S. Koda: *Jpn. J. Appl. Phys.* **48** (2009) 07GA09.
- 11) K. Sakai, T. Hirano, and M. Hosoda: *Appl. Phys. Express* **3** (2010) 016602.
- 12) L. D. Landau and E. M. Lifshitz: *Fluid Mechanics* (Butterworth-Heinemann, Oxford, U.K., 1989) Chap. 2.
- 13) M. Hosoda, K. Sakai, and K. Takagi: *Phys. Rev. E* **58** (1998) 6275.